Neuroimaging Biomarkers in Alzheimer's Disease and Related Disorders

Joseph C. Masdeu and Belen Pascual

Abbreviations

^{18}F-FDG	^{18}F-2-deoxy-2-fluoro-D-glucose
AD	Alzheimer's disease
Amyloid	Beta-amyloid
APOE	Apolipoprotein E
ASL	Arterial spin labeling
CSF	Cerebrospinal fluid
CT	Computed tomography
FDA	US Food and Drug Administration
FLAIR	Fluid-attenuated inversion recovery
fMRI	Functional magnetic resonance imaging
FTD	Frontotemporal dementia
LBD	Lewy body dementia
lvPPA	Logopenic aphasia
MCI	Mild cognitive impairment
MRI	Magnetic resonance imaging
nfvPPA	Non-fluent primary progressive aphasia
PET	Positron-emission tomography
PPA	Primary progressive aphasia
PSP	Progressive supranuclear palsy
ROC	Receiver operating characteristic

J. C. Masdeu (✉) · B. Pascual
Nantz National Alzheimer Center, Houston Methodist Stanley H. Appel Department of Neurology and Weill Cornell Medicine, Houston, TX, USA
e-mail: jcmasdeu@houstonmethodist.org

A. L. Teixeira et al. (eds.), *Biomarkers in Neuropsychiatry*,
https://doi.org/10.1007/978-3-031-43356-6_11

SPECT	Single photon emission computed tomography
svFTD	Semantic variant of frontotemporal dementia
Tau	Hyperphosphorylated tau
TSPO	Translocator protein

1 Introduction

The 2018 Research Framework defined the beta-amyloid, tau, and neurodegeneration or AT[N] stages, determined by imaging biomarkers, as critical for Alzheimer's disease (AD) research [1]. Imaging biomarkers for AD were used mostly in research until June 2021, when the US Food and Drug Administration (FDA) approved aducanumab for clinical use; since then, imaging biomarkers have been used in the clinic as well as in research because amyloid deposition in the brain needs to be documented before aducanumab may be used. Under the commercial name Aduhelm™, aducanumab is a human monoclonal antibody that selectively reacts with beta-amyloid brain aggregates, including soluble oligomers and insoluble fibrils [2]. Beta-amyloid (amyloid for brevity) is a protein that begins to accumulate in the brain of people who eventually will develop AD 5–15 years before the onset of clinical symptoms [3]. While amyloid imaging showed that aducanumab reduced brain amyloid in clinical trials including patients with mild cognitive impairment (MCI) and mild AD [4], the reduction in clinical worsening associated with AD was minimally or not affected by aducanumab at the clinical stages included in these trials [4, 5]. Nonetheless, physicians began prescribing this medication, which logically required demonstrating amyloid brain accumulation in a potential candidate for aducanumab therapy. While abnormal brain amyloid can be predicted by measuring amyloid and tau in cerebrospinal fluid [6], people prefer amyloid imaging when availability or cost does not preclude its use. Although the use of plasma biomarkers of amyloid deposition in the brain is promising and gaining in accuracy [7], at the time of this writing either CSF or imaging is still needed to document brain amyloid deposition in the clinic [8]. Brain amyloid removal by monoclonal antibodies occurs largely through the walls of small vessels, which become more permeable, giving rise to brain edema or microhemorrhages in about 25% of the treated patients [9]. The occurrence of both events can be monitored with MRI using the FLAIR sequence for edema and gradient echo or susceptibility-weighted sequences to monitor blood deposition in the brain [9].

The clinical use of imaging biomarkers was further encouraged by the January 2023 FDA approval of lecanemab (Leqembi™), another humanized monoclonal antibody, this one targeting soluble amyloid protofibrils and causing not only a reduction of brain amyloid but also a slowing of the clinical worsening as well [10]. That the clinical effect was modest could be explained by the stage of AD at which this medication was used. In mice, two broad stages can be observed, an *amyloid-dependent* stage and an *amyloid-independent* stage [11]. When excess amyloid is removed from the brain at the amyloid-dependent stage, the animals do not go on to

develop Alzheimer's disease. However, if excess amyloid is removed at the amyloid-independent stage, the animals continue to worsen relentlessly until death. At the amyloid-dependent stage, there is no abnormal tau in the brain of the animals, but at the amyloid-dependent stage, abnormal, phosphorylated tau has begun to be detectable in the brain [11]. Similar changes can be observed in humans using imaging biomarkers [12]. The brain deposition of amyloid alone is not associated with cognitive impairment [3]. However, when tau is detected by imaging outside the entorhinal cortex, people are already symptomatic, with the degree and type of clinical symptoms correlating closely with the degree of tau deposition and its location in the brain [13]. Areas with high tau are typically hypometabolic on FDG PET, such that there is a ying-yang relationship between these two imaging biomarkers: where tau is high, metabolism is low (Fig. 1). As both aducanumab and lecanemab were in clinical trials of symptomatic subjects, who were likely at the amyloid-independent stage, even the modest clinical effect is encouraging. From the foregoing, determining tau build up in the brain of a potential candidate for one of these therapies could be very helpful to predict benefit: people with more tau are less likely to benefit from anti-amyloid antibodies [14].

At the time of this writing, several monoclonal antibodies targeting brain amyloid are being studied at the pre-symptomatic, amyloid-dependent, stage. These studies are made possible by the availability of amyloid imaging to detect excess brain amyloid in people who are cognitively unimpaired. Furthermore, although neuropsychological scores are used as outcome measures, brain tau provides a measure with less day-to-day variability than neuropsychological testing, and it is beginning to be used as an outcome measure [15]. This chapter will review the imaging biomarkers mentioned in this introduction and others most extensively used in dementia, leaving for future reviews potentially useful biomarkers, for instance, cortical mean diffusivity [16].

2 Neuroimaging Biomarkers

The imaging modalities used to study AD include MRI and PET. Single photon emission computed tomography (SPECT) is also being used to study brain perfusion, but its use has been largely replaced by the use of an MRI sequence, arterial spin labelling, that allows for the study of brain perfusion.

2.1 MRI Regional Brain Volume

Neurodegeneration causes progressive loss of brain volume, which cannot be appreciated on MRI images nearly as well as other brain lesions, such as tumors or infarction. Although brain volume loss, widely known as atrophy, can be rated visually [17], automated methods are less time-consuming and more precise and facilitate

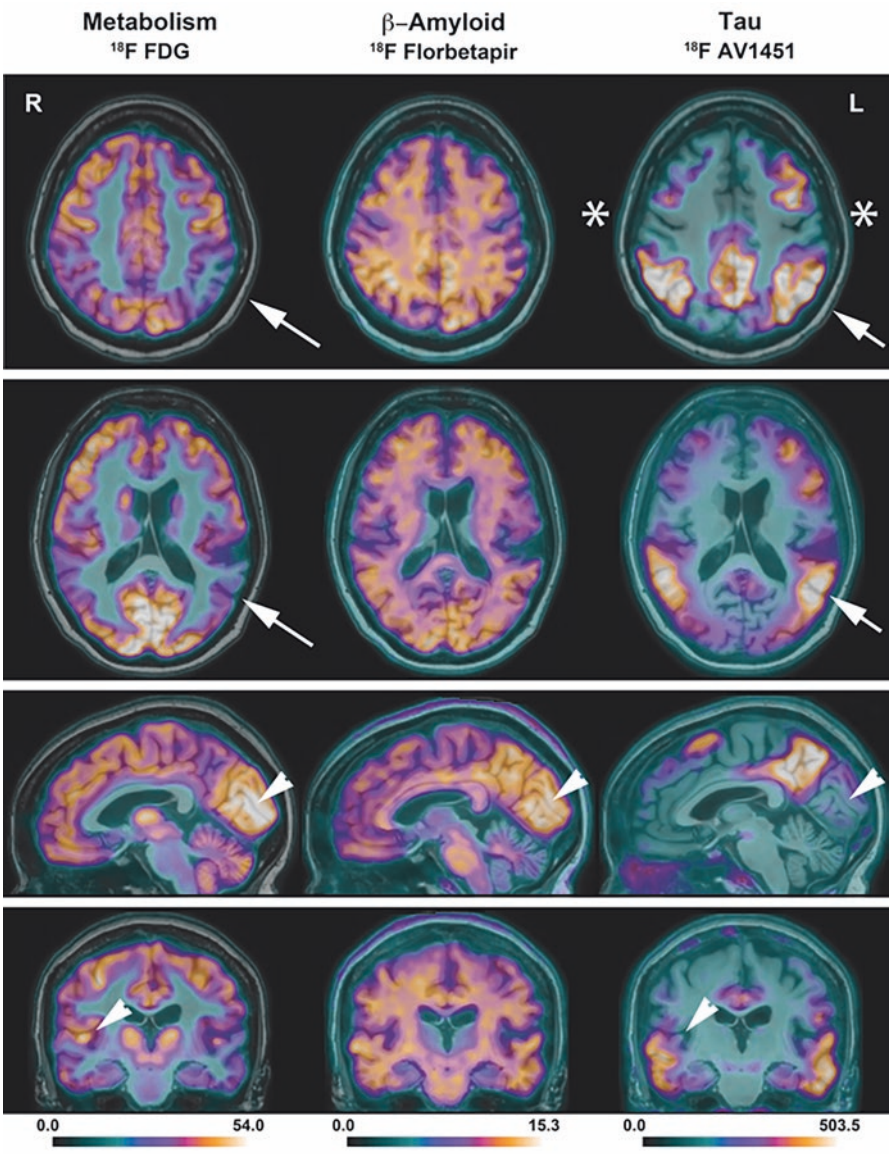

Fig. 1 Imaging findings in patient with AD (logopenic aphasia). Metabolism, amyloid, and tau imaging from a 57-year-old woman with the logopenic aphasia variety of Alzheimer's disease. The primary sensory-motor areas (asterisks), as well as the primary visual (striatal cortex) and auditory (Heschl's gyrus) regions (arrowheads), have normal metabolism and no tau deposition. By contrast, areas with a high tau deposition (e.g., inferior parietal lobule, arrows) tend to have decreased metabolism. In some areas, a high amyloid deposition corresponds to a low metabolism and an increased tau (e.g., the precuneus). However, there are areas with high amyloid load and normal metabolism, such as the medial occipital region. Uptake in the region of the substantia nigra does not correspond to tau deposition. (From [13] with permission)

longitudinal follow-up. Classical automated methods follow one of the two approaches: voxel-based morphometry (VBM) [18] or surface-based morphometry (SBM) [19–21]. These methods are based on the automatic segmentation of the brain cortex, deep nuclei, white matter, and ventricles, based on the different intensities of these structures, mostly on T1-weighted images. In VBM, through sophisticated deformation techniques, beyond the scope of this chapter, the brain of a given individual is placed in a standard brain template, thus facilitating the statistical comparison of the various brain regions of this individual with similar regions of a control sample, typically healthy people of similar age and sex as the individual of interest [22, 23]. In SBM, similar procedures are used for segmentation of the various components of the brain, but the boundary between the cortical gray and underlying white matter is obtained. This boundary, together with surface coordinates of the brain of the individual of interest, as well as its deep structures, is ingeniously compared to standard brains and atlases that contain the typical anatomical regions [24, 25]. The first SBM software, FreeSurfer [26, 27], which is available through an open access license, is perhaps the volumetric software most commonly used in research. For clinical use, several VBM or SBM commercial packages are available for seamless integration with clinical PACS systems. In dementia MRI, the accuracy of software that classifies clinically appropriate cases has been compared favorably with the accuracy of trained readers [28]. Interestingly, even among image specialists, those with more experience in reading brain images obtain the best clinical results in dementia patients from automated MRI volume methods [29]. More recently, machine learning and neural network computing are revolutionizing the use of MRI and other imaging datasets for the longitudinal assessment of brain changes in AD/ADRD [30–33]. Since the steps of data processing are not as clear as with VBM or SBM, the reliability of these techniques can be best evaluated by researchers with an extensive knowledge of brain anatomy and function and by comparison with other quantitative techniques [34].

Volume loss in the medial temporal regions was the first reliable neuroimaging finding detected in AD [35] and still thought to be the most robust on MRI. The name of *neurodegenerative pattern* has been assigned to the pattern of atrophy most often observed in AD [36] (Fig. 2). Indeed, regional atrophy in a set of mostly post-Rolandic structures is a strong predictor of AD on MRI [19]. In cognitively unimpaired people, the presence of a neurodegenerative MRI pattern is predictive of the development of mild cognitive impairment later in life, particularly when associated with amyloid deposition [37].

Most cortical thickness studies have assumed a linear volume loss in the AD process, starting at the pre-symptomatic stages. However, a biphasic pattern is more likely, with increased thickness at some point of the very early process, followed by subsequent progressive thinning [38, 39]. This pattern would agree with early inflammatory changes resulting in cortical swelling that would be compensated for and surpassed by the volume loss caused by later progressive neuronal loss. This pattern would explain why atrophy has not been found by every study to predate the onset of cognitive impairment in familial autosomal dominant AD [40–43]. It would also explain the paradoxical increased "atrophy" in patients treated with

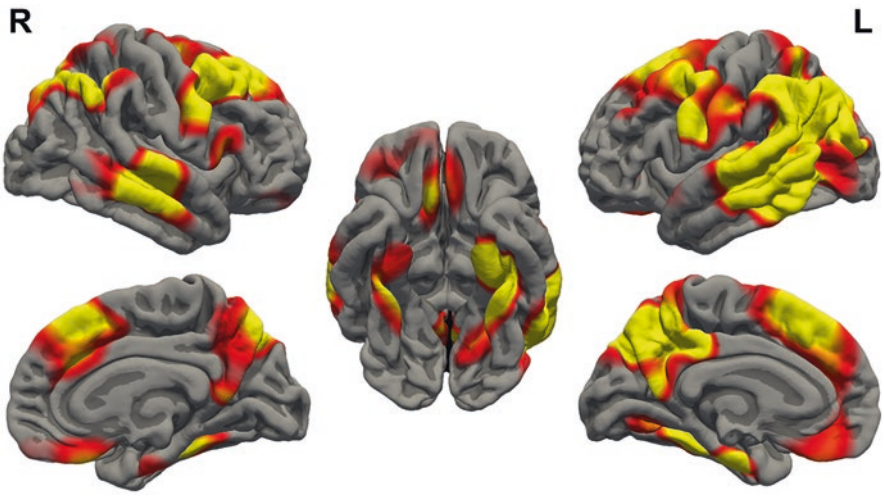

Fig. 2 Cortical thickness in Alzheimer's disease. On MRI templates of the brain, in color are areas of the brain of a patient with Alzheimer's disease where the cortex is thinner at a higher (yellow) or lower (red) statistical level as compared to a group of controls of the same age and sex

monoclonal antibodies targeting amyloid [44]. A reduction in cortical amyloid has been documented neuropathologically to reduce inflammation in the cortex [45]. These data suggest that MRI volumetry is not a reliable marker of neurodegeneration in therapeutic trials.

By correlating postmortem findings with the pattern of atrophy on MRI, three distinct atrophy patterns have been found in patients with typical AD neuropathology, including amyloid deposition: typical AD (about 70% of cases), limbic-predominant AD (20%) and hippocampal-sparing AD (10%) [46]. Most patients with typical and limbic-predominant AD initially present with an amnestic syndrome, but only about 40% of those with hippocampal-sparing AD do. Medial temporal atrophy is most severe in patients with limbic-predominant AD, followed closely by typical AD, and milder in those with hippocampal-sparing AD. Conversely, the most severe cortical atrophy was noted in patients with hippocampal-sparing AD, followed by those with typical disease, and then limbic-predominant AD. The ratio of hippocampal to cortical volumes allowed the best discrimination between subtypes [46]. In addition, some AD patients, particularly younger ones, present with a disorder of visual perception, including one or several components of Balint's syndrome, alexia, and even field defects on confrontation testing, caused by posterior cortical atrophy [47–49] (Fig. 3).

The pattern of atrophy in AD resembles that of dementia with Lewy bodies (DLB) [50], but in DLB there is more atrophy in the fusiform gyrus and paracentral cortex [51]. The imaging similarity between the two diseases can be explained at least in part by the frequent coexistence of AD and alpha-synuclein neuropathologies [50,

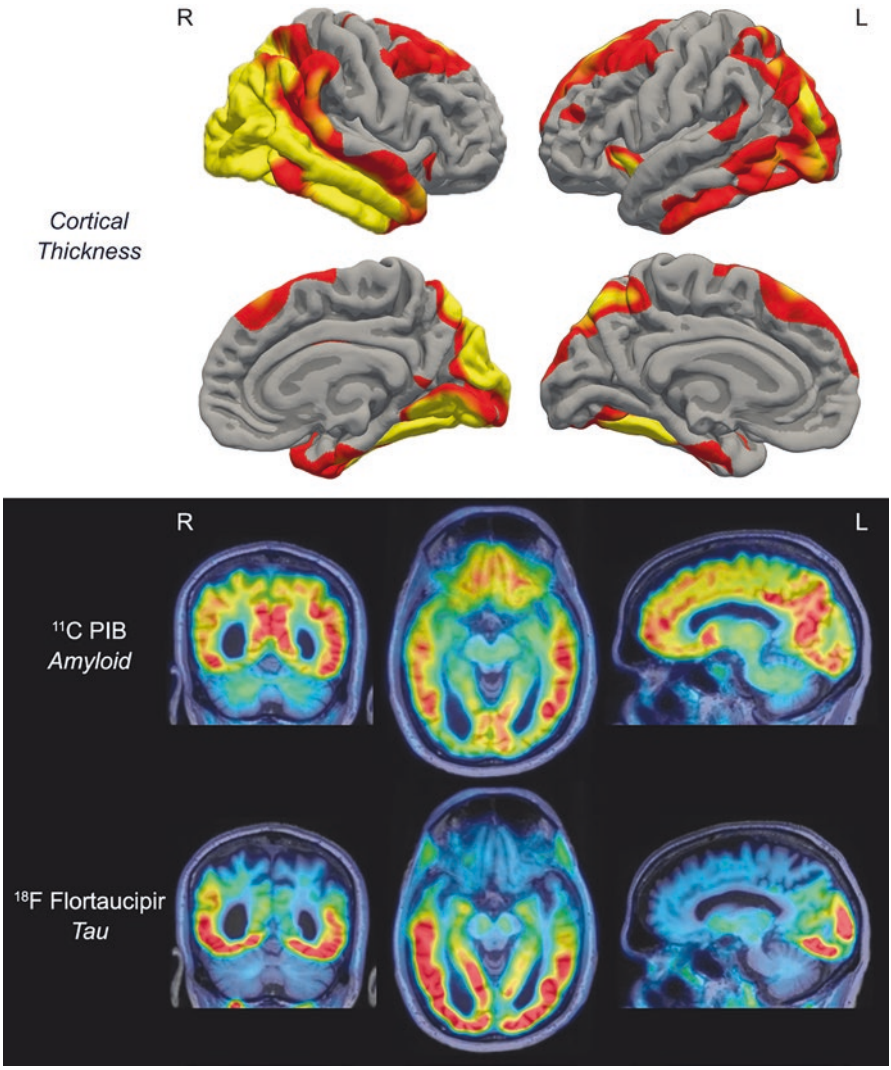

Fig. 3 Cortical thickness, amyloid, and tau in a patient with the posterior cortical atrophy variant of Alzheimer's disease. Areas of decreased cortical thickness are indicated as in Fig 2. Areas with increased amyloid or tau are in red. Note the similar topography of these changes, most pronounced in the posterior portion of the brain

52, 53]. Patients with pure alpha-synuclein pathology have little atrophy, such that the lack of hippocampal atrophy associated with memory loss in MCI is indicative of DLB [54]. Atrophy in AD, which tends to affect the posterior brain regions, differs from atrophy in FTD, which tends to affect the anterior portion of the brain [55]. Hippocampal volume alone poorly differentiates AD from FTD; hippocampal sclerosis associated with FTD could explain the overlap [56].

2.2 Metabolism

Regional brain metabolism is currently used as a biomarker of neurodegeneration, for instance, to document the "N," neurodegeneration, in the AT[N] system [1]. Metabolism is measured with ^{18}F-FDG PET [57–59]. Metabolism may be closely linked to the pathophysiology of AD; as in older people, the regional brain expression of AD-risk genes correlates with regional metabolism [60]. The most typical metabolic pattern found in early AD is decreased metabolism bilaterally in the parietotemporal association cortex and posterior cingulate gyrus [61] (Fig. 4). Metabolism reflects synaptic activity and therefore is most affected early in the regions to which medial temporal neurons project [62, 63] and may reflect impaired connectivity even in pre-symptomatic subjects [40, 64]. As atrophy corresponds to neuronal loss, it is no surprise that the regions most affected on volumetric MRI and metabolic PET do not coincide early in AD [65], but they partially overlap as the disease progresses [66]. As AD progresses, some areas of the frontal association cortex become hypometabolic, while the paracentral cortex (primary motor-sensory areas) remains preserved (Fig. 1). The specificity and sensitivity of these findings continue to be debated. In studies of AD with neuropathological confirmation, the sensitivity (84–95%) has been higher than the specificity (71–74%), that is, a normal study is seldom associated with AD [59, 67]. Using consensus diagnosis, in an area under the receiver operating characteristic (ROC) analysis for three automated approaches to mild AD diagnosis, the specificity approximates 85% when the

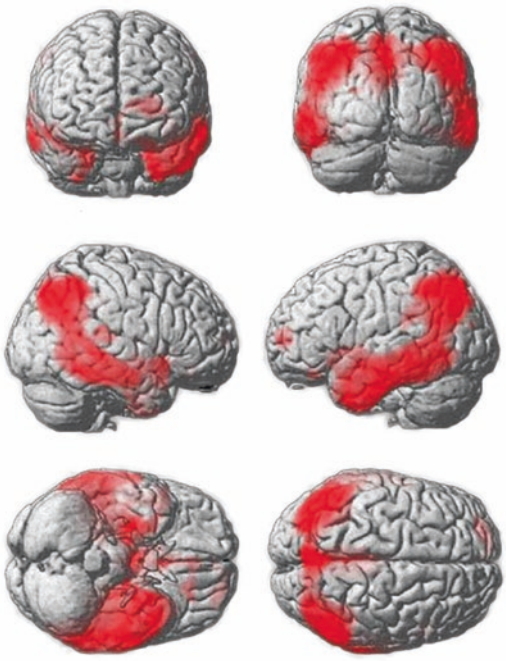

Fig. 4 FDG PET group findings in Alzheimer's disease. Projected on a rendered MRI and shown in red are areas with a low metabolism in a group of 28 patients with early Alzheimer's disease, compared with 28 healthy controls. Note sparing of the paracentral (primary motor-sensory) cortex

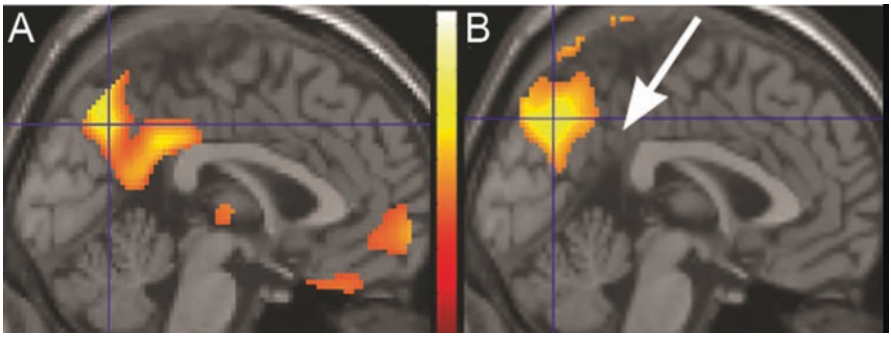

Fig. 5 "Island sign" in Lewy body dementia (LBD). On MRI templates of the medial aspect of the brain, areas of decreased metabolism (^{18}F-FDG PET) in AD (**A**) and decreased perfusion ($H_2{}^{15}O$-PET) in LBD (**B**). Metabolism and perfusion are coupled in AD and LBD. Note involvement of the posterior cingulate gyrus in AD but sparing of this region (arrow) in LBD. (Modified from [153])

sensitivity is pegged at 80% [68]. Depending on the approach and the sample studied, the accuracy for predicting the evolution of MCI to AD varies from 0.774 to 0.983 [68]. Among persons with MCI, those most likely to progress to AD have metabolic findings similar to AD [69]. ^{18}F-FDG PET may predict better than structural MRI or SPECT the worsening from MCI to AD [70].

The AD metabolic pattern can also be found with DLB, in part because the two brain pathologies often coexist [52, 53]. However, while AD tends to render hypometabolic the posterior cingulate gyrus, this structure is often spared in DLB, giving rise to the "posterior-cingulate island sign" on FDG PET [71] (Fig. 5). Unlike AD, which tends to affect posterior brain regions, the frontal and anterior portions of the temporal lobes are usually hypometabolic in FTD [58]. Patients with progranulin mutations, however, often have parietal involvement [72].

2.3 Perfusion Imaging

In the absence of associated vascular disease [73], perfusion is typically coupled to metabolism in neurodegenerative disorders. In current clinical practice, brain perfusion is most often studied with MRI arterial spin labelling (ASL), a sequence that can be obtained together with more conventional MRI sequences. As expected, cerebral blood flow (CBF) obtained with ASL tends to correlate topographically with metabolism, particularly in the more advanced AD stages [74–78]. However, FDG PET slightly outperforms ASL in separating AD and, particularly, MCI patients from controls, both in visual readings and using automated procedures [74, 77, 79, 80].

Brain perfusion can also be assessed with SPECT, using Tc-99m HMPAO (hexamethyl propylamine oxime, Ceretec™), a lipid soluble macrocyclic amine, or

Tc-99m ECD (ethyl cysteinate dimer, Neurolite™). A head-to-head comparison of perfusion SPECT with metabolism PET has shown better sensitivity and specificity of PET over SPECT in AD and diffuse Lewy body disease [57].

2.4 Amyloid Imaging

Brain amyloid was initially imaged with "Pittsburgh compound B" (^{11}C-PIB) [81]. PIB is available bound to ^{11}C, a positron-emitting isotope with a half-life of 20.4 min, requiring an on-site cyclotron. However, since 2012 there are amyloid-imaging compounds bound to ^{18}F, with a half-life of 109.8 min. The longer half-life allows for the radiotracer to be synthesized at a facility with a cyclotron and then shipped to institutions with PET cameras, more widely available. Good concordance with histologically measured amyloid load has been shown not only for PIB [82, 83] but also for three ^{18}F amyloid PET tracers, ^{18}F-florbetapir [84], ^{18}F-flutemetamol [85], and ^{18}F-florbetaben [86], which are approved by the FDA for use in the clinical setting. At the time of this writing, 2023, a fourth amyloid PET tracer, ^{18}F-flutafuranol, also known as ^{18}F-NAV4694, is only used in research, but it has much less white-matter binding than other ^{18}F tracers, thus providing cleaner images, similar to those obtained with PIB [87].

As another biomarker of AD, decreased CSF amyloid 42 [88], amyloid brain deposition begins in the preclinical stages of AD, increases during the MCI stage, and, by the time of the AD diagnosis, remains relatively stable as the disease progresses [3, 89]. Thus, amyloid deposition is a marker of the pre-symptomatic stages of the disease and correlates with the degree of cognitive impairment only in the preclinical stages and MCI, not during AD [3, 90], while atrophy and synaptic dysfunction continue to increase and spread as clinical AD worsens and cognition deteriorates [89].

In asymptomatic individuals of similar age, amyloid deposition has been found more often among *APOE*4 carriers [91], but this genotype may not have an effect on the risk of cognitive worsening once its effect on amyloid deposition is accounted for [92, 93]. Lifetime cognitive engagement has been found to protect from preclinical amyloid deposition [94], but this effect, like the protective effect of physical exercise, may be restricted to *APOE*4 carriers [95]. Impaired sleep has been associated with an increased amyloid burden [96].

Amyloid deposition is the strongest and earliest neuroimaging predictor of future cognitive impairment in healthy elderly and of worsening from MCI to AD, increasing the risk between three- and sevenfold [92, 97, 98]. The effect of amyloid deposition on cognitive impairment in the early stages of the AD continuum may be modulated by some common genetic variants. For instance, healthy *APOE4* carriers have not only a greater amyloid deposition but also worse memory and visuospatial skills for the same amount of 11C-PIB binding [99]. This finding may reflect a longer period of time with amyloid deposition in the APOE4 carriers. Healthy, amyloid-positive carriers of the Met genotype of the brain-derived neurotrophic factor

(BDNF) *Val66Met* allele have a greater worsening on follow-up in episodic memory, language, and executive function than the Val homozygotes despite similar amyloid PET binding in both groups [100].

Amyloid imaging is also a powerful tool to separate the dementias characterized by amyloid deposition, such as AD and diffuse DLB, often associated with AD [53], from the FTD, which course without amyloid deposition. Separating patient samples of AD and FTD validated clinically, areas under the ROC curve for 11C-PIB (0.888) and ^{18}F-FDG (0.910) were similar [101]. 11C-PIB slightly outperformed ^{18}F-FDG in patients with known histopathology [101]. A confounder is the presence of amyloid deposition in some older people with FTD because the prevalence of amyloid positivity increases with age [37, 102]. Although the diagnosis of AD is predicated on the presence of amyloid plaques in the brain [103], a few cases with AD have a tau PET typical for AD, with intense uptake in the cortex of AD regions, but a negative amyloid PET [104, 105]. Neuropathology is still lacking, but it is possible that these patients have diffuse or cotton-wool plaques or some other type of amyloid burden not well imaged with the current amyloid PET tracers [106, 107]. These patients should not be confused with patients who have a negative amyloid PET, but a positive signal, although typically weaker than in AD, in FTD-typical areas with one of the tau tracers. In these cases, the signal is often greatest in white matter, which on neuropathology contains a lower density of known abnormal protein aggregates, such as tau or TDP-43, than the cortex [108].

Patients with an AD clinical phenotype may have a negative amyloid PET scan. In a clinical trial of early AD, 14% had negative amyloid scans among 214 with AD symptomatology [109]. This proportion parallels the 14% amyloid-negative in a population sample of 154 amnesic MCI patients and 16% of 58 MCI patients from ADNI [110] and may rise to 30% when the patients studied are older than 82 years [111]. It may reflect the smaller subset of patients with dementia who do not have elevated amyloid or tau at autopsy [112]. These imaging findings could reflect the rather mixed pathology found in the oldest-old [113]. However, even with a careful neuropathological exclusion of other etiologies, clinical and neuropathological findings are occasionally dissociated: individuals with marked amyloid and neurofibrillary pathology may be cognitively intact [112]. In these individuals there is less amyloid deposition in the form of fibrillar plaques and intimately related oligomeric amyloid assemblies, less hyperphosphorylated soluble tau species localized in synapses, and less glial activation [114].

In early AD, amyloid deposition is highest in the default network and, thus, in fronto-parieto-temporal association cortex, including the precuneus, but sparing the paracentral regions and primary visual and auditory sensory cortex (Fig. 1). The caudate nucleus is often affected as well.

Longitudinal amyloid imaging allows for the evaluation of the natural history of amyloid deposition among at-risk genotypes [91], and it is being used as a marker of effectiveness in clinical trials carried out during the preclinical stage of AD, because it has helped elucidate brain changes during AD therapy [10, 115, 116].

2.5 *Tau Imaging*

In the healthy brain, the protein tau stabilizes neurotubules and is therefore essential for normal neural function [11]. However, in AD and other neurodegenerative disorders, tau becomes abnormally hyperphosphorylated, dysfunctional, and misfolded, constituting the tangles observed neuropathologically in AD and other tauopathies. PET tracers are available that bind strongly to the abnormally folded tau, using the folding properties of this protein for binding. These tracers do not bind to the healthy, native form of tau, but here we refer to hyperphosphorylated tau simply as "tau," as has become common usage. PET tracers currently used to image tau include ^{18}F-T807, most recently known as ^{18}F-AV-1451 or ^{18}F-flortaucipir [117–119], which was approved for clinical use by the FDA after a postmortem study proved that ^{18}F-flortaucipir binds to tau tangles in AD [120]. ^{18}F-Flortaucipir shows highly specific uptake in areas known neuropathologically to contain a large amount of tau in AD [13, 118, 121] (Fig. 1). It has little white matter binding, but there is uptake in the substantia nigra, explained by binding of ^{18}F-flortaucipir to melanin [122, 123], and in the choroid plexus, possibly from binding to calcifications or even tau in this structure [124, 125]. In older individuals, even those cognitively intact, there is nonspecific binding in the lenticular nucleus, red nucleus, and subthalamic nucleus, possibly due to iron deposition [124], as well as in the upper portion of the cerebellum (Fig. 6).

^{18}F-Flortaucipir binds to tau in AD [126], which is associated with 3- and 4-repeat (3R and 4R) tau aggregates, but much less or not at all with 3R or 4R tau found in most varieties of tau-related FTD [122, 124]. The configuration of tau aggregates, which differs in various tauopathies [127], most likely determines binding. For instance, ^{18}F-flortaucipir binds to patients harboring a p.R406W mutation in the *MAPT* gene, encoding tau [128]. This mutation results in 3R and 4R tau aggregates

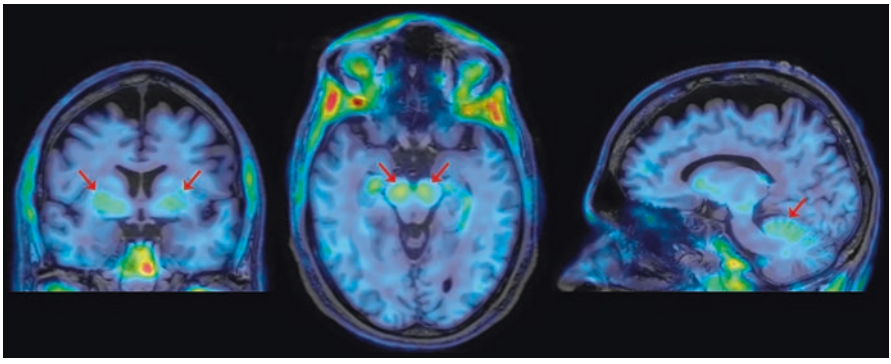

Fig. 6 "Nonspecific" uptake with the PET tau tracer ^{18}F-flortaucipir. From left to right and projected on MRI, coronal, axial, and sagittal ^{18}F-flortaucipir images from a cognitively normal 72-year-old man. Note uptake in the globus pallidus (coronal section, white arrows), substantia nigra (axial section, arrows), and superior portion of the cerebellum (sagittal section, arrow). None of these areas are known to harbor tau

like those in AD [128]. ^{18}F-Flortaucipir also binds weakly to the regions most affected in FTD cases and, particularly, in semantic dementia [129], but careful neuropathological evaluation has shown a lack of binding to 4R tau or to TDP-43 [124, 130, 131]. Furthermore, the signal in FTD involves the white matter, rather than the cortex, where the accumulation of misfolded proteins is greatest [108]. This binding has been postulated to correspond to MAO-B, abundantly expressed by astrocytes, but the ^{18}F-flortaucipir signal has not been suppressed by blocking MAO-B [108].

Compared to ^{18}F-flortaucipir, two commonly used newer tau PET tracers have less nonspecific binding to the lenticular nucleus, ^{18}F-MK6240 and ^{18}F-PI-2620. There is extensive experience with ^{18}F-MK6240, which has less binding to choroid plexus than ^{18}F-flortaucipir, thus allowing for a better quantification of tau deposition in medial temporal regions, including the entorhinal cortex [105]. A negative characteristic of ^{18}F-MK6240 is the frequent intense binding to meningeal structures and to the skull (Fig. 7); various methods have been suggested to compensate for this binding [132]. Less experience exists with ^{18}F-PI-2620, which also seems to bind to the meninges and skull [133]. ^{18}F-PI-2620 has been postulated to bind not only to AD tau [134] but also to 4R tau as well and thus be useful in imaging corticobasal degeneration and progressive supranuclear palsy [133, 135].

Tau accumulation measured with tau PET tracers correlates better with the degree of cognitive impairment than amyloid accumulation [136], a finding in agreement with prior neuropathological studies [137]. Furthermore, there is an inverse correlation between tau accumulation and brain metabolism: regions high in tau have uniformly depressed metabolism [13] (Fig. 1). This correlation is not as tight with amyloid accumulation (Fig. 1).

In amyloid-negative, clinically normal people older than 60, tau accumulation in the entorhinal cortex is associated with worse cognitive performance and greater tau in other brain regions [138].

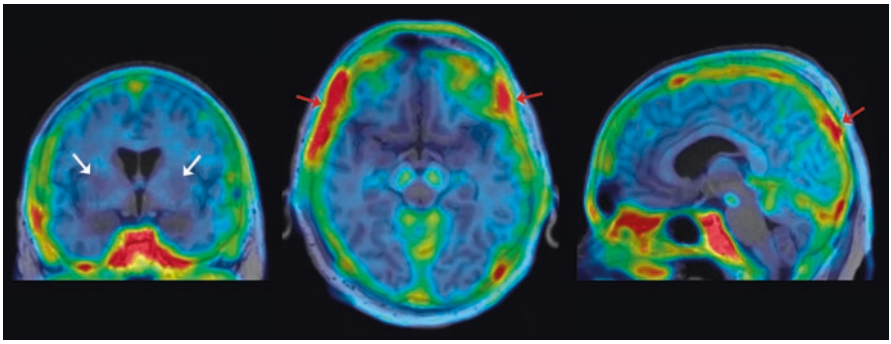

Fig. 7 "Nonspecific" uptake with the PET tau tracer ^{18}F-MK6240. From left to right and projected on MRI, coronal, axial, and sagittal ^{18}F-MK6240 images from a cognitively normal 73-year-old man. Please compare it with Fig. 6. Although there is no uptake in the globus pallidus (coronal section, white arrows), there is still uptake in the substantia nigra and uptake in the skull and meninges (red arrows)

2.6 Inflammation Imaging

Although brain inflammation is prominent in AD and related disorders, the use of inflammation imaging is not as widespread as that of previously described imaging biomarkers. Inflammation can be pathogenic, reflect scavenging of neurons and neuronal processes, or have a neuroprotective effect [139–141]. Animal models of tau-induced neuronal loss have shown earlier and more severe inflammation than models of increased amyloid [142], and both microglia and reactive astrocytes are found at autopsy to be increased in areas of the brain affected by neurodegenerative pathology. However, in vivo brain inflammation data in human neurodegeneration is scant. PET imaging allows in vivo quantification of neuroinflammation by measuring the density of the 18-kDa translocator protein (TSPO), which is expressed in microglia, astrocytes, and reactive endothelial cells. TSPO has been imaged with ^{11}C-PK11195, a compound that in humans has a low affinity for the receptor [143] and a low ratio of specific-to-nonspecific binding [144]. The limitations of ^{11}C-PK11195 prompted the development of second-generation radioligands for imaging activated microglia. ^{11}C-PBR28 is a second-generation radioligand with a high affinity to TSPO, favorable in vivo kinetics, and greater signal-to-noise ratio than ^{11}C-PK11195 in monkey brain [144]. Unfortunately, the affinity of this and other TSPO PET tracers is strongly determined by the rs6971 polymorphism on the *TSPO* gene, leading to high- and low-affinity groups, as well as an intermediate phenotype. More recently developed, ^{11}C-ER176 has a higher affinity for TSPO and allows for imaging of people with the low-affinity rs6971 polymorphism of the *TSPO* gene [145, 146].

Using these tracers, increased brain inflammation has been documented even at pre-symptomatic stages of AD [147], with a good topographic correlation between inflammation and amyloid deposition (Fig. 8). At the MCI stage, many studies, for instance [148, 149], but not all [150] have shown neuroinflammation. The lack of consistency at the MCI stage may be related to a biphasic effect of inflammation, with earlier and later peaks [151], possibly neuroprotective at the early stages, but harmful at later stages. While this is still unclear, neuroinflammation seems to mediate tau spreading [152]. In dementing diseases more focal than AD, such as semantic dementia, inflammation has been shown to peak at the boundary between involved and healthy brain (Fig. 9), suggesting that inflammation plays an important role in the progression of neurodegeneration [108].

In conclusion, the availability of imaging biomarkers for several of the major components of AD has greatly furthered the understanding of the development of this disease in humans. Furthermore, it has facilitated the performance of clinical trials that have recently yielded positive results. In terms of imaging, the development of tracers for alpha-synuclein and TDP-43, of great importance in LBD and FTD respectively, is being worked on. Furthermore, perfecting plasma biomarkers would greatly facilitate population screening, so that putative therapies could be applied to prevent or thwart the pathological processes causing irreparable neuronal loss in diseases leading to dementia.

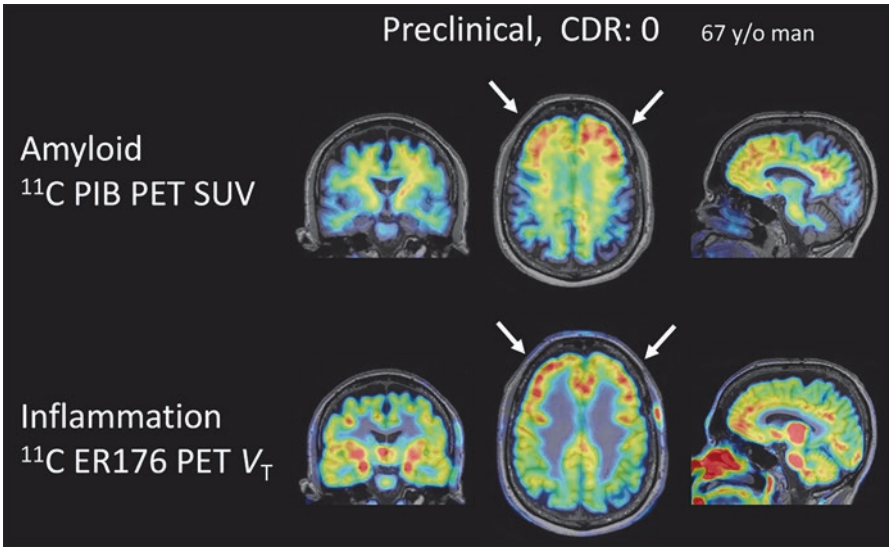

Fig. 8 Amyloid and inflammation PET in a pre-symptomatic AD patient. Although this person was cognitively unimpaired, amyloid PET evidenced increased amyloid deposition in the frontal lobe and precuneus. Similar regions had inflammation on ^{11}C-ER176 PET. This tracer binds to TSPO

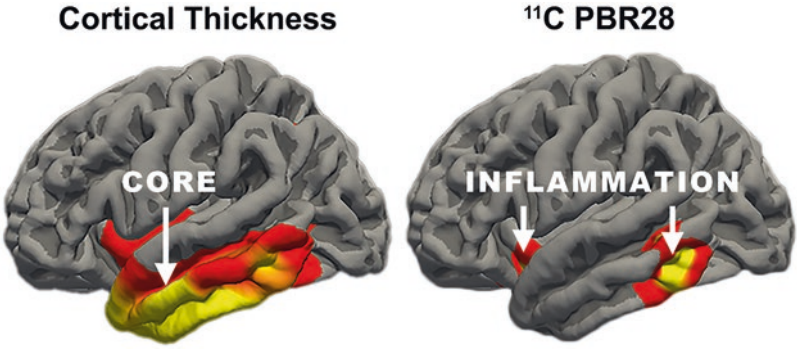

Fig. 9 Cortical thickness on MRI and inflammation PET in semantic dementia. On brain templates, in color are areas where a group of patients with semantic dementia differ from controls. Cortical thickness is most abnormal at the anterior portion of the left temporal lobe, in the core of the damage, while inflammation peaks at the periphery of the area with reduced cortical thickness. (From [108])

Funding This work was supported by the Nantz National Alzheimer Center, Houston Methodist Neurological Institute, and by the Chao, Baucom, Graham, Harrison, Henning and Nantz Funds from the Houston Methodist Hospital Foundation, as well as by the Dearing.

References

1. Jack CR Jr, Bennett DA, Blennow K, Carrillo MC, Dunn B, Haeberlein SB, Holtzman DM, Jagust W, Jessen F, Karlawish J, Liu E, Molinuevo JL, Montine T, Phelps C, Rankin KP, Rowe CC, Scheltens P, Siemers E, Snyder HM, Sperling R, Contributors. NIA-AA Research Framework: toward a biological definition of Alzheimer's disease. Alzheimers Dement. 2018;14:535–62.
2. Sevigny J, Chiao P, Bussiere T, Weinreb PH, Williams L, Maier M, Dunstan R, Salloway S, Chen T, Ling Y, O'Gorman J, Qian F, Arastu M, Li M, Chollate S, Brennan MS, Quintero-Monzon O, Scannevin RH, Arnold HM, Engber T, Rhodes K, Ferrero J, Hang Y, Mikulskis A, Grimm J, Hock C, Nitsch RM, Sandrock A. The antibody aducanumab reduces abeta plaques in Alzheimer's disease. Nature. 2016;537:50–6.
3. Villemagne VL, Pike KE, Chetelat G, Ellis KA, Mulligan RS, Bourgeat P, Ackermann U, Jones G, Szoeke C, Salvado O, Martins R, O'Keefe G, Mathis CA, Klunk WE, Ames D, Masters CL, Rowe CC. Longitudinal assessment of Abeta and cognition in aging and Alzheimer disease. Ann Neurol. 2011;69:181–92.
4. Budd Haeberlein S, Aisen PS, Barkhof F, Chalkias S, Chen T, Cohen S, Dent G, Hansson O, Harrison K, von Hehn C, Iwatsubo T, Mallinckrodt C, Mummery CJ, Muralidharan KK, Nestorov I, Nisenbaum L, Rajagovindan R, Skordos L, Tian Y, van Dyck CH, Vellas B, Wu S, Zhu Y, Sandrock A. Two randomized phase 3 studies of aducanumab in early Alzheimer's disease. J Prev Alzheimers Dis. 2022;9:197–210.
5. Costa T, Cauda F. A Bayesian reanalysis of the phase III aducanumab (ADU) trial. J Alzheimers Dis. 2022;87:1009–12.
6. Barthélemy NR, Saef B, Li Y, Gordon BA, He Y, Horie K, Stomrud E, Salvadó G, Janelidze S, Sato C, Ovod V, Henson RL, Fagan AM, Benzinger TLS, Xiong C, Morris JC, Hansson O, Bateman RJ, Schindler SE. CSF tau phosphorylation occupancies at T217 and T205 represent improved biomarkers of amyloid and tau pathology in Alzheimer's disease. Nat Aging. 2023;3:391–401.
7. Jack CR, Wiste HJ, Algeciras-Schimnich A, Figdore DJ, Schwarz CG, Lowe VJ, Ramanan VK, Vemuri P, Mielke MM, Knopman DS, Graff-Radford J, Boeve BF, Kantarci K, Cogswell PM, Senjem ML, Gunter JL, Therneau TM, Petersen RC. Predicting amyloid PET and tau PET stages with plasma biomarkers. Brain. 2023;146:2029–44.
8. Mattsson-Carlgren N, Palmqvist S. The emerging era of staging Alzheimer's disease pathology using plasma biomarkers. Brain. 2023;146:1740–2.
9. Salloway S, Chalkias S, Barkhof F, Burkett P, Barakos J, Purcell D, Suhy J, Forrestal F, Tian Y, Umans K, Wang G, Singhal P, Budd Haeberlein S, Smirnakis K. Amyloid-related imaging abnormalities in 2 phase 3 studies evaluating aducanumab in patients with early Alzheimer disease. JAMA Neurol. 2022;79:13–21.
10. van Dyck CH, Swanson CJ, Aisen P, Bateman RJ, Chen C, Gee M, Kanekiyo M, Li D, Reyderman L, Cohen S, Froelich L, Katayama S, Sabbagh M, Vellas B, Watson D, Dhadda S, Irizarry M, Kramer LD, Iwatsubo T. Lecanemab in early Alzheimer's disease. N Engl J Med. 2023;388:9–21.
11. Hyman BT. Amyloid-dependent and amyloid-independent stages of Alzheimer disease. Arch Neurol. 2011;68:1062–4.
12. Masdeu JC, Pascual B. Genetic and degenerative disorders primarily causing dementia. Handb Clin Neurol. 2016;135:525–64.

13. Pascual B, Masdeu JC. Tau, amyloid, and hypometabolism in the logopenic variant of primary progressive aphasia. Neurology. 2016;86:487–8.
14. Reardon S. Alzheimer's drug donanemab: what promising trial means for treatments. Nature. 2023;617:232–3.
15. Shcherbinin S, Evans CD, Lu M, Andersen SW, Pontecorvo MJ, Willis BA, Gueorguieva I, Hauck PM, Brooks DA, Mintun MA, Sims JR. Association of amyloid reduction after donanemab treatment with tau pathology and clinical outcomes: the TRAILBLAZER-ALZ randomized clinical trial. JAMA Neurol. 2022;79:1015–24.
16. Rodriguez-Vieitez E, Montal V, Sepulcre J, Lois C, Hanseeuw B, Vilaplana E, Schultz AP, Properzi MJ, Scott MR, Amariglio R, Papp KV, Marshall GA, Fortea J, Johnson KA, Sperling RA, Vannini P. Association of cortical microstructure with amyloid-β and tau: impact on cognitive decline, neurodegeneration, and clinical progression in older adults. Mol Psychiatry. 2021;26:7813–22.
17. Scheltens P, Fox N, Barkhof F, De Carli C. Structural magnetic resonance imaging in the practical assessment of dementia: beyond exclusion. Lancet Neurol. 2002;1:13–21.
18. Good CD, Scahill RI, Fox NC, Ashburner J, Friston KJ, Chan D, Crum WR, Rossor MN, Frackowiak RS. Automatic differentiation of anatomical patterns in the human brain: validation with studies of degenerative dementias. NeuroImage. 2002;17:29–46.
19. Dickerson BC, Bakkour A, Salat DH, Feczko E, Pacheco J, Greve DN, Grodstein F, Wright CI, Blacker D, Rosas HD, Sperling RA, Atri A, Growdon JH, Hyman BT, Morris JC, Fischl B, Buckner RL. The cortical signature of Alzheimer's disease: regionally specific cortical thinning relates to symptom severity in very mild to mild AD dementia and is detectable in asymptomatic amyloid-positive individuals. Cereb Cortex. 2009;19:497–510.
20. Thompson PM, Hayashi KM, de Zubicaray G, Janke AL, Rose SE, Semple J, Herman D, Hong MS, Dittmer SS, Doddrell DM, Toga AW. Dynamics of gray matter loss in Alzheimer's disease. J Neurosci. 2003;23:994–1005.
21. Goto M, Abe O, Hagiwara A, Fujita S, Kamagata K, Hori M, Aoki S, Osada T, Konishi S, Masutani Y, Sakamoto H, Sakano Y, Kyogoku S, Daida H. Advantages of using both voxel- and surface-based morphometry in cortical morphology analysis: a review of various applications. Magn Reson Med Sci. 2022;21:41–57.
22. Ashburner J. A fast diffeomorphic image registration algorithm. NeuroImage. 2007;38:95–113.
23. Ashburner J, Friston KJ. Voxel-based morphometry – the methods. NeuroImage. 2000;11:805–21.
24. Fischl B, Sereno MI, Dale AM. Cortical surface-based analysis. II: inflation, flattening, and a surface-based coordinate system. NeuroImage. 1999;9:195–207.
25. Fischl B, Sereno MI, Tootell RB, Dale AM. High-resolution intersubject averaging and a coordinate system for the cortical surface. Hum Brain Mapp. 1999;8:272–84.
26. Fischl B, Salat DH, Busa E, Albert M, Dieterich M, Haselgrove C, van der Kouwe A, Killiany R, Kennedy D, Klaveness S, Montillo A, Makris N, Rosen B, Dale AM. Whole brain segmentation: automated labeling of neuroanatomical structures in the human brain. Neuron. 2002;33:341–55.
27. Fischl B. FreeSurfer. https://surfer.nmr.mgh.harvard.edu/, 2023.
28. Kloppel S, Stonnington CM, Barnes J, Chen F, Chu C, Good CD, Mader I, Mitchell LA, Patel AC, Roberts CC, Fox NC, Jack CR Jr, Ashburner J, Frackowiak RS. Accuracy of dementia diagnosis: a direct comparison between radiologists and a computerized method. Brain. 2008;131:2969–74.
29. Pemberton HG, Goodkin O, Prados F, Das RK, Vos SB, Moggridge J, Coath W, Gordon E, Barrett R, Schmitt A, Whiteley-Jones H, Burd C, Wattjes MP, Haller S, Vernooij MW, Harper L, Fox NC, Paterson RW, Schott JM, Bisdas S, White M, Ourselin S, Thornton JS, Yousry TA, Cardoso MJ, Barkhof F. Automated quantitative MRI volumetry reports support diagnostic interpretation in dementia: a multi-rater, clinical accuracy study. Eur Radiol. 2021;31:5312–23.

30. Balboni E, Nocetti L, Carbone C, Dinsdale N, Genovese M, Guidi G, Malagoli M, Chiari A, Namburete AIL, Jenkinson M, Zamboni G. The impact of transfer learning on 3D deep learning convolutional neural network segmentation of the hippocampus in mild cognitive impairment and Alzheimer disease subjects. Hum Brain Mapp. 2022;43:3427–38.
31. Joo L, Shim WH, Suh CH, Lim SJ, Heo H, Kim WS, Hong E, Lee D, Sung J, Lim JS, Lee JH, Kim SJ. Diagnostic performance of deep learning-based automatic white matter hyperintensity segmentation for classification of the Fazekas scale and differentiation of subcortical vascular dementia. PLoS One. 2022;17:e0274562.
32. Liu S, Masurkar AV, Rusinek H, Chen J, Zhang B, Zhu W, Fernandez-Granda C, Razavian N. Generalizable deep learning model for early Alzheimer's disease detection from structural MRIs. Sci Rep. 2022;12:17106.
33. Martí-Juan G, Lorenzi M, Piella G. MC-RVAE: multi-channel recurrent variational autoencoder for multimodal Alzheimer's disease progression modelling. NeuroImage. 2023;268:119892.
34. Lee J, Burkett BJ, Min HK, Senjem ML, Lundt ES, Botha H, Graff-Radford J, Barnard LR, Gunter JL, Schwarz CG, Kantarci K, Knopman DS, Boeve BF, Lowe VJ, Petersen RC, Jack CR Jr, Jones DT. Deep learning-based brain age prediction in normal aging and dementia. Nat Aging. 2022;2:412–24.
35. Masdeu J, Aronson M. CT findings in early dementia. The Gerontologist. 1985;25:82.
36. Jack CR Jr, Knopman DS, Chetelat G, Dickson D, Fagan AM, Frisoni GB, Jagust W, Mormino EC, Petersen RC, Sperling RA, van der Flier WM, Villemagne VL, Visser PJ, Vos SJ. Suspected non-Alzheimer disease pathophysiology – concept and controversy. Nat Rev Neurol. 2016;12:117–24.
37. Petersen RC, Lundt ES, Therneau TM, Weigand SD, Knopman DS, Mielke MM, Roberts RO, Lowe VJ, Machulda MM, Kremers WK, Geda YE, Jack CR Jr. Predicting progression to mild cognitive impairment. Ann Neurol. 2019;85:155–60.
38. Montal V, Vilaplana E, Pegueroles J, Bejanin A, Alcolea D, Carmona-Iragui M, Clarimón J, Levin J, Cruchaga C, Graff-Radford NR, Noble JM, Lee JH, Allegri R, Karch CM, Laske C, Schofield PR, Salloway S, Ances B, Benzinger T, McDale E, Bateman R, Blesa R, Sánchez-Valle R, Lleó A, Fortea J. Biphasic cortical macro- and microstructural changes in autosomal dominant Alzheimer's disease. Alzheimers Dement. 2021;17:618–28.
39. Fortea J, Sala-Llonch R, Bartres-Faz D, Bosch B, Llado A, Bargallo N, Molinuevo JL, Sanchez-Valle R. Increased cortical thickness and caudate volume precede atrophy in PSEN1 mutation carriers. J Alzheimers Dis. 2010;22:909–22.
40. Yau WY, Tudorascu DL, McDade EM, Ikonomovic S, James JA, Minhas D, Mowrey W, Sheu LK, Snitz BE, Weissfeld L, Gianaros PJ, Aizenstein HJ, Price JC, Mathis CA, Lopez OL, Klunk WE. Longitudinal assessment of neuroimaging and clinical markers in autosomal dominant Alzheimer's disease: a prospective cohort study. Lancet Neurol. 2015;14:804–13.
41. Bateman RJ, Xiong C, Benzinger TL, Fagan AM, Goate A, Fox NC, Marcus DS, Cairns NJ, Xie X, Blazey TM, Holtzman DM, Santacruz A, Buckles V, Oliver A, Moulder K, Aisen PS, Ghetti B, Klunk WE, McDade E, Martins RN, Masters CL, Mayeux R, Ringman JM, Rossor MN, Schofield PR, Sperling RA, Salloway S, Morris JC. Clinical and biomarker changes in dominantly inherited Alzheimer's disease. N Engl J Med. 2012;367:795–804.
42. Reiman EM, Quiroz YT, Fleisher AS, Chen K, Velez-Pardo C, Jimenez-Del-Rio M, Fagan AM, Shah AR, Alvarez S, Arbelaez A, Giraldo M, Acosta-Baena N, Sperling RA, Dickerson B, Stern CE, Tirado V, Munoz C, Reiman RA, Huentelman MJ, Alexander GE, Langbaum JB, Kosik KS, Tariot PN, Lopera F. Brain imaging and fluid biomarker analysis in young adults at genetic risk for autosomal dominant Alzheimer's disease in the presenilin 1 E280A kindred: a case-control study. Lancet Neurol. 2012;11:1048–56.
43. Apostolova LG, Hwang KS, Medina LD, Green AE, Braskie MN, Dutton RA, Lai J, Geschwind DH, Cummings JL, Thompson PM, Ringman JM. Cortical and hippocampal atrophy in patients with autosomal dominant familial Alzheimer's disease. Dement Geriatr Cogn Disord. 2011;32:118–25.

44. Salloway S, Sperling R, Fox NC, Blennow K, Klunk W, Raskind M, Sabbagh M, Honig LS, Porsteinsson AP, Ferris S, Reichert M, Ketter N, Nejadnik B, Guenzler V, Miloslavsky M, Wang D, Lu Y, Lull J, Tudor IC, Liu E, Grundman M, Yuen E, Black R, Brashear HR, Bapineuzumab, Clinical Trial I. Two phase 3 trials of bapineuzumab in mild-to-moderate Alzheimer's disease. N Engl J Med. 2014;370:322–33.
45. Zotova E, Bharambe V, Cheaveau M, Morgan W, Holmes C, Harris S, Neal JW, Love S, Nicoll JA, Boche D. Inflammatory components in human Alzheimer's disease and after active amyloid-beta42 immunization. Brain. 2013;136:2677–96.
46. Whitwell JL, Dickson DW, Murray ME, Weigand SD, Tosakulwong N, Senjem ML, Knopman DS, Boeve BF, Parisi JE, Petersen RC, Jack CR Jr, Josephs KA. Neuroimaging correlates of pathologically defined subtypes of Alzheimer's disease: a case-control study. Lancet Neurol. 2012;11:868–77.
47. Ossenkoppele R, Schonhaut DR, Baker SL, O'Neil JP, Janabi M, Ghosh PM, Santos M, Miller ZA, Bettcher BM, Gorno-Tempini ML, Miller BL, Jagust WJ, Rabinovici GD. Tau, amyloid, and hypometabolism in a patient with posterior cortical atrophy. Ann Neurol. 2015;77:338–42.
48. Lehmann M, Ghosh PM, Madison C, Laforce R Jr, Corbetta-Rastelli C, Weiner MW, Greicius MD, Seeley WW, Gorno-Tempini ML, Rosen HJ, Miller BL, Jagust WJ, Rabinovici GD. Diverging patterns of amyloid deposition and hypometabolism in clinical variants of probable Alzheimer's disease. Brain. 2013;136:844–58.
49. Rosenbloom MH, Alkalay A, Agarwal N, Baker SL, O'Neil JP, Janabi M, Yen IV, Growdon M, Jang J, Madison C, Mormino EC, Rosen HJ, Gorno-Tempini ML, Weiner MW, Miller BL, Jagust WJ, Rabinovici GD. Distinct clinical and metabolic deficits in PCA and AD are not related to amyloid distribution. Neurology. 2011;76:1789–96.
50. Nedelska Z, Ferman TJ, Boeve BF, Przybelski SA, Lesnick TG, Murray ME, Gunter JL, Senjem ML, Vemuri P, Smith GE, Geda YE, Graff-Radford J, Knopman DS, Petersen RC, Parisi JE, Dickson DW, Jack CR Jr, Kantarci K. Pattern of brain atrophy rates in autopsy-confirmed dementia with Lewy bodies. Neurobiol Aging. 2015;36:452–61.
51. Ye R, Touroutoglou A, Brickhouse M, Katz S, Growdon JH, Johnson KA, Dickerson BC, Gomperts SN. Topography of cortical thinning in the Lewy body diseases. Neuroimage Clin. 2020;26:102196.
52. Boyle PA, Yu L, Leurgans SE, Wilson RS, Brookmeyer R, Schneider JA, Bennett DA. Attributable risk of Alzheimer's dementia attributed to age-related neuropathologies. Ann Neurol. 2019;85:114–24.
53. Toledo JB, Gopal P, Raible K, Irwin DJ, Brettschneider J, Sedor S, Waits K, Boluda S, Grossman M, Van Deerlin VM, Lee EB, Arnold SE, Duda JE, Hurtig H, Lee VM, Adler CH, Beach TG, Trojanowski JQ. Pathological α-synuclein distribution in subjects with coincident Alzheimer's and Lewy body pathology. Acta Neuropathol. 2016;131:393–409.
54. Kantarci K, Lesnick T, Ferman TJ, Przybelski SA, Boeve BF, Smith GE, Kremers WK, Knopman DS, Jack CR Jr, Petersen RC. Hippocampal volumes predict risk of dementia with Lewy bodies in mild cognitive impairment. Neurology. 2016;87:2317–23.
55. Whitwell JL, Boeve BF, Weigand SD, Senjem ML, Gunter JL, Baker MC, DeJesus-Hernandez M, Knopman DS, Wszolek ZK, Petersen RC, Rademakers R, Jack CR Jr, Josephs KA. Brain atrophy over time in genetic and sporadic frontotemporal dementia: a study of 198 serial magnetic resonance images. Eur J Neurol. 2015;22:745–52.
56. de Souza LC, Chupin M, Bertoux M, Lehericy S, Dubois B, Lamari F, Le Ber I, Bottlaender M, Colliot O, Sarazin M. Is hippocampal volume a good marker to differentiate Alzheimer's disease from frontotemporal dementia? J Alzheimers Dis. 2013;36:57–66.
57. O'Brien JT, Firbank MJ, Davison C, Barnett N, Bamford C, Donaldson C, Olsen K, Herholz K, Williams D, Lloyd J. 18F-FDG PET and perfusion SPECT in the diagnosis of Alzheimer and Lewy body dementias. J Nucl Med. 2014;55:1959–65.
58. Herholz K. Guidance for reading FDG PET scans in dementia patients. Q J Nucl Med Mol Imaging. 2014;58:332–43.

59. Jagust W, Reed B, Mungas D, Ellis W, Decarli C. What does fluorodeoxyglucose PET imaging add to a clinical diagnosis of dementia? Neurology. 2007;69:871–7.
60. Ye F, Funk Q, Rockers E, Shulman JM, Masdeu JC, Pascual B. In Alzheimer-prone brain regions, metabolism and risk-gene expression are strongly correlated. Brain Commun. 2022;4:fcac216.
61. Chen K, Ayutyanont N, Langbaum JB, Fleisher AS, Reschke C, Lee W, Liu X, Bandy D, Alexander GE, Thompson PM, Shaw L, Trojanowski JQ, Jack CR Jr, Landau SM, Foster NL, Harvey DJ, Weiner MW, Koeppe RA, Jagust WJ, Reiman EM, Alzheimer's Disease Neuroimaging I. Characterizing Alzheimer's disease using a hypometabolic convergence index. NeuroImage. 2011;56:52–60.
62. Miettinen PS, Pihlajamaki M, Jauhiainen AM, Niskanen E, Hanninen T, Vanninen R, Soininen H. Structure and function of medial temporal and posteromedial cortices in early Alzheimer's disease. Eur J Neurosci. 2011;34:320–30.
63. Bozoki AC, Korolev IO, Davis NC, Hoisington LA, Berger KL. Disruption of limbic white matter pathways in mild cognitive impairment and Alzheimer's disease: a DTI/FDG-PET study. Hum Brain Mapp. 2011;33(8):1792–802.
64. Drzezga A, Becker JA, Van Dijk KR, Sreenivasan A, Talukdar T, Sullivan C, Schultz AP, Sepulcre J, Putcha D, Greve D, Johnson KA, Sperling RA. Neuronal dysfunction and disconnection of cortical hubs in non-demented subjects with elevated amyloid burden. Brain. 2011;134:1635–46.
65. Chetelat G, Desgranges B, Landeau B, Mezenge F, Poline JB, de la Sayette V, Viader F, Eustache F, Baron JC. Direct voxel-based comparison between grey matter hypometabolism and atrophy in Alzheimer's disease. Brain. 2008;131:60–71.
66. La Joie R, Perrotin A, Barre L, Hommet C, Mezenge F, Ibazizene M, Camus V, Abbas A, Landeau B, Guilloteau D, de La Sayette V, Eustache F, Desgranges B, Chetelat G. Region-specific hierarchy between atrophy, hypometabolism, and beta-amyloid (Abeta) load in Alzheimer's disease dementia. J Neurosci. 2012;32:16265–73.
67. Silverman DH, Small GW, Chang CY, Lu CS, Kung De Aburto MA, Chen W, Czernin J, Rapoport SI, Pietrini P, Alexander GE, Schapiro MB, Jagust WJ, Hoffman JM, Welsh-Bohmer KA, Alavi A, Clark CM, Salmon E, de Leon MJ, Mielke R, Cummings JL, Kowell AP, Gambhir SS, Hoh CK, Phelps ME. Positron emission tomography in evaluation of dementia: regional brain metabolism and long-term outcome. JAMA. 2001;286:2120–7.
68. Caroli A, Prestia A, Chen K, Ayutyanont N, Landau SM, Madison CM, Haense C, Herholz K, Nobili F, Reiman EM, Jagust WJ, Frisoni GB, Eadc-Pet Consortium N-D, Alzheimer's Disease Neuroimaging I. Summary metrics to assess Alzheimer disease-related hypometabolic pattern with 18F-FDG PET: head-to-head comparison. J Nucl Med. 2012;53:592–600.
69. Mosconi L, Brys M, Glodzik-Sobanska L, De Santi S, Rusinek H, de Leon MJ. Early detection of Alzheimer's disease using neuroimaging. Exp Gerontol. 2007;42:129–38.
70. Yuan Y, Gu ZX, Wei WS. Fluorodeoxyglucose-positron-emission tomography, single-photon emission tomography, and structural MR imaging for prediction of rapid conversion to Alzheimer disease in patients with mild cognitive impairment: a meta-analysis. AJNR Am J Neuroradiol. 2009;30:404–10.
71. Graff-Radford J, Murray ME, Lowe VJ, Boeve BF, Ferman TJ, Przybelski SA, Lesnick TG, Senjem ML, Gunter JL, Smith GE, Knopman DS, Jack CR Jr, Dickson DW, Petersen RC, Kantarci K. Dementia with Lewy bodies: basis of cingulate Island sign. Neurology. 2014;83:801–9.
72. Josephs KA, Duffy JR, Strand EA, Machulda MM, Vemuri P, Senjem ML, Perkerson RB, Baker MC, Lowe V, Jack CR Jr, Rademakers R, Whitwell JL. Progranulin-associated PiB-negative logopenic primary progressive aphasia. J Neurol. 2014;261:604–14.
73. Wong CY, Thie J, Gaskill M, Ponto R, Hill J, Tian HY, Balon H, Wu D, Fink-Bennett D, Nagle C. A statistical investigation of normal regional intra-subject heterogeneity of brain metabolism and perfusion by F-18 FDG and O-15 H2O PET imaging. BMC Nucl Med. 2006;6:4.

74. Dolui S, Li Z, Nasrallah IM, Detre JA, Wolk DA. Arterial spin labeling versus (18)F-FDG-PET to identify mild cognitive impairment. Neuroimage Clin. 2020;25:102146.
75. Yan L, Liu CY, Wong KP, Huang SC, Mack WJ, Jann K, Coppola G, Ringman JM, Wang DJJ. Regional association of pCASL-MRI with FDG-PET and PiB-PET in people at risk for autosomal dominant Alzheimer's disease. Neuroimage Clin. 2018;17:751–60.
76. Verclytte S, Lopes R, Lenfant P, Rollin A, Semah F, Leclerc X, Pasquier F, Delmaire C. Cerebral hypoperfusion and hypometabolism detected by arterial spin labeling MRI and FDG-PET in early-onset Alzheimer's disease. J Neuroimaging. 2016;26:207–12.
77. Tosun D, Schuff N, Jagust W, Weiner MW. Discriminative power of arterial spin labeling magnetic resonance imaging and 18F-fluorodeoxyglucose positron emission tomography changes for amyloid-β-positive subjects in the Alzheimer's disease continuum. Neurodegener Dis. 2016;16:87–94.
78. Verfaillie SC, Adriaanse SM, Binnewijzend MA, Benedictus MR, Ossenkoppele R, Wattjes MP, Pijnenburg YA, van der Flier WM, Lammertsma AA, Kuijer JP, Boellaard R, Scheltens P, van Berckel BN, Barkhof F. Cerebral perfusion and glucose metabolism in Alzheimer's disease and frontotemporal dementia: two sides of the same coin? Eur Radiol. 2015;25:3050–9.
79. Ceccarini J, Bourgeois S, Van Weehaeghe D, Goffin K, Vandenberghe R, Vandenbulcke M, Sunaert S, Van Laere K. Direct prospective comparison of (18)F-FDG PET and arterial spin labelling MR using simultaneous PET/MR in patients referred for diagnosis of dementia. Eur J Nucl Med Mol Imaging. 2020;47:2142–54.
80. Riederer I, Bohn KP, Preibisch C, Wiedemann E, Zimmer C, Alexopoulos P, Förster S. Alzheimer disease and mild cognitive impairment: integrated pulsed arterial spin-labeling MRI and (18)F-FDG PET. Radiology. 2018;288:198–206.
81. Klunk WE, Koeppe RA, Price JC, Benzinger TL, Devous MD Sr, Jagust WJ, Johnson KA, Mathis CA, Minhas D, Pontecorvo MJ, Rowe CC, Skovronsky DM, Mintun MA. The Centiloid Project: standardizing quantitative amyloid plaque estimation by PET. Alzheimers Dement. 2015;11(1–15):e11–4.
82. Villeneuve S, Rabinovici GD, Cohn-Sheehy BI, Madison C, Ayakta N, Ghosh PM, La Joie R, Arthur-Bentil SK, Vogel JW, Marks SM, Lehmann M, Rosen HJ, Reed B, Olichney J, Boxer AL, Miller BL, Borys E, Jin LW, Huang EJ, Grinberg LT, DeCarli C, Seeley WW, Jagust W. Existing Pittsburgh Compound-B positron emission tomography thresholds are too high: statistical and pathological evaluation. Brain. 2015;138:2020–33.
83. Murray ME, Lowe VJ, Graff-Radford NR, Liesinger AM, Cannon A, Przybelski SA, Rawal B, Parisi JE, Petersen RC, Kantarci K, Ross OA, Duara R, Knopman DS, Jack CR Jr, Dickson DW. Clinicopathologic and 11C-Pittsburgh compound B implications of Thal amyloid phase across the Alzheimer's disease spectrum. Brain. 2015;138:1370–81.
84. Choi SR, Schneider JA, Bennett DA, Beach TG, Bedell BJ, Zehntner SP, Krautkramer MJ, Kung HF, Skovronsky DM, Hefti F, Clark CM. Correlation of amyloid PET ligand florbetapir F 18 binding with abeta aggregation and neuritic plaque deposition in postmortem brain tissue. Alzheimer Dis Assoc Disord. 2012;26:8–16.
85. Wolk DA, Grachev ID, Buckley C, Kazi H, Grady MS, Trojanowski JQ, Hamilton RH, Sherwin P, McLain R, Arnold SE. Association between in vivo fluorine 18-labeled flutemetamol amyloid positron emission tomography imaging and in vivo cerebral cortical histopathology. Arch Neurol. 2011;68:1398–403.
86. Sabri O, Sabbagh MN, Seibyl J, Barthel H, Akatsu H, Ouchi Y, Senda K, Murayama S, Ishii K, Takao M, Beach TG, Rowe CC, Leverenz JB, Ghetti B, Ironside JW, Catafau AM, Stephens AW, Mueller A, Koglin N, Hoffmann A, Roth K, Reininger C, Schulz-Schaeffer WJ. Florbetaben PET imaging to detect amyloid beta plaques in Alzheimer's disease: phase 3 study. Alzheimers Dement. 2015;11:964–74.
87. Rowe CC, Jones G, Dore V, Pejoska S, Margison L, Mulligan RS, Chan JG, Young K, Villemagne VL. Standardized expression of 18F-NAV4694 and 11C-PiB beta-amyloid PET results with the centiloid scale. J Nucl Med. 2016;57:1233–7.

88. Palmqvist S, Zetterberg H, Mattsson N, Johansson P, Minthon L, Blennow K, Olsson M, Hansson O. Detailed comparison of amyloid PET and CSF biomarkers for identifying early Alzheimer disease. Neurology. 2015;85:1240–9.
89. Jack CR Jr, Lowe VJ, Senjem ML, Weigand SD, Kemp BJ, Shiung MM, Knopman DS, Boeve BF, Klunk WE, Mathis CA, Petersen RC. 11C PiB and structural MRI provide complementary information in imaging of Alzheimer's disease and amnestic mild cognitive impairment. Brain. 2008;131:665–80.
90. Chetelat G, Villemagne VL, Pike KE, Ellis KA, Ames D, Masters CL, Rowe CC. Relationship between memory performance and beta-amyloid deposition at different stages of Alzheimer's disease. Neurodegener Dis. 2012;10:141–4.
91. Vlassenko AG, Mintun MA, Xiong C, Sheline YI, Goate AM, Benzinger TL, Morris JC. Amyloid-beta plaque growth in cognitively normal adults: longitudinal [11C]Pittsburgh compound B data. Ann Neurol. 2011;70:857–61.
92. Petersen RC, Wiste HJ, Weigand SD, Rocca WA, Roberts RO, Mielke MM, Lowe VJ, Knopman DS, Pankratz VS, Machulda MM, Geda YE, Jack CR Jr. Association of elevated amyloid levels with cognition and biomarkers in cognitively normal people from the community. JAMA Neurol. 2016;73:85–92.
93. Lim YY, Laws SM, Villemagne VL, Pietrzak RH, Porter T, Ames D, Fowler C, Rainey-Smith S, Snyder PJ, Martins RN, Salvado O, Bourgeat P, Rowe CC, Masters CL, Maruff P. Abeta-related memory decline in APOE epsilon4 noncarriers: implications for Alzheimer disease. Neurology. 2016;86:1635–42.
94. Landau SM, Marks SM, Mormino EC, Rabinovici GD, Oh H, O'Neil JP, Wilson RS, Jagust WJ. Association of lifetime cognitive engagement and low beta-amyloid deposition. Arch Neurol. 2012;69:623–9.
95. Vemuri P, Lesnick TG, Przybelski SA, Knopman DS, Machulda M, Lowe VJ, Mielke MM, Roberts RO, Gunter JL, Senjem ML, Geda YE, Rocca WA, Petersen RC, Jack CR Jr. Effect of intellectual enrichment on AD biomarker trajectories: longitudinal imaging study. Neurology. 2016;86:1128–35.
96. Brown BM, Rainey-Smith SR, Villemagne VL, Weinborn M, Bucks RS, Sohrabi HR, Laws SM, Taddei K, Macaulay SL, Ames D, Fowler C, Maruff P, Masters CL, Rowe CC, Martins RN. The relationship between sleep quality and brain amyloid burden. Sleep. 2016;39:1063–8.
97. Burnham SC, Bourgeat P, Dore V, Savage G, Brown B, Laws S, Maruff P, Salvado O, Ames D, Martins RN, Masters CL, Rowe CC, Villemagne VL. Clinical and cognitive trajectories in cognitively healthy elderly individuals with suspected non-Alzheimer's disease pathophysiology (SNAP) or Alzheimer's disease pathology: a longitudinal study. Lancet Neurol. 2016;15:1044–53.
98. Schreiber S, Landau SM, Fero A, Schreiber F, Jagust WJ. Comparison of visual and quantitative florbetapir F 18 positron emission tomography analysis in predicting mild cognitive impairment outcomes. JAMA Neurol. 2015;72:1183–90.
99. Kantarci K, Lowe V, Przybelski SA, Weigand SD, Senjem ML, Ivnik RJ, Preboske GM, Roberts R, Geda YE, Boeve BF, Knopman DS, Petersen RC, Jack CR Jr. APOE modifies the association between Abeta load and cognition in cognitively normal older adults. Neurology. 2012;78:232–40.
100. Lim YY, Villemagne VL, Laws SM, Ames D, Pietrzak RH, Ellis KA, Harrington KD, Bourgeat P, Salvado O, Darby D, Snyder PJ, Bush AI, Martins RN, Masters CL, Rowe CC, Nathan PJ, Maruff P. BDNF Val66Met, Abeta amyloid, and cognitive decline in preclinical Alzheimer's disease. Neurobiol Aging. 2013;34:2457–64.
101. Rabinovici GD, Rosen HJ, Alkalay A, Kornak J, Furst AJ, Agarwal N, Mormino EC, O'Neil JP, Janabi M, Karydas A, Growdon ME, Jang JY, Huang EJ, Dearmond SJ, Trojanowski JQ, Grinberg LT, Gorno-Tempini ML, Seeley WW, Miller BL, Jagust WJ. Amyloid vs FDG-PET in the differential diagnosis of AD and FTLD. Neurology. 2011;77:2034–42.
102. Serrano GE, Sabbagh MN, Sue LI, Hidalgo JA, Schneider JA, Bedell BJ, Van Deerlin VM, Suh E, Akiyama H, Joshi AD, Pontecorvo MJ, Mintun MA, Beach TG. Positive florbetapir

PET amyloid imaging in a subject with frequent cortical neuritic plaques and frontotemporal lobar degeneration with TDP43-positive inclusions. J Alzheimers Dis. 2014;42:813–21.
103. Hyman BT, Phelps CH, Beach TG, Bigio EH, Cairns NJ, Carrillo MC, Dickson DW, Duyckaerts C, Frosch MP, Masliah E, Mirra SS, Nelson PT, Schneider JA, Thal DR, Thies B, Trojanowski JQ, Vinters HV, Montine TJ. National Institute on Aging-Alzheimer's Association guidelines for the neuropathologic assessment of Alzheimer's disease. Alzheimers Dement. 2012;8:1–13.
104. Krishnadas N, Doré V, Laws SM, Porter T, Lamb F, Bozinovski S, Villemagne VL, Rowe CC. Exploring discordant low amyloid beta and high neocortical tau positron emission tomography cases. Alzheimers Dement (Amst). 2022;14:e12326.
105. Pascoal TA, Therriault J, Benedet AL, Savard M, Lussier FZ, Chamoun M, Tissot C, Qureshi MNI, Kang MS, Mathotaarachchi S, Stevenson J, Hopewell R, Massarweh G, Soucy JP, Gauthier S, Rosa-Neto P. 18F-MK-6240 PET for early and late detection of neurofibrillary tangles. Brain. 2020;143:2818–30.
106. Abrahamson EE, Kofler JK, Becker CR, Price JC, Newell KL, Ghetti B, Murrell JR, McLean CA, Lopez OL, Mathis CA, Klunk WE, Villemagne VL, Ikonomovic MD. 11C-PiB PET can underestimate brain amyloid-β burden when cotton wool plaques are numerous. Brain. 2022;145:2161–76.
107. Ikonomovic MD, Buckley CJ, Abrahamson EE, Kofler JK, Mathis CA, Klunk WE, Farrar G. Post-mortem analyses of PiB and flutemetamol in diffuse and cored amyloid-β plaques in Alzheimer's disease. Acta Neuropathol. 2020;140:463–76.
108. Pascual B, Funk Q, Zanotti-Fregonara P, Cykowski MD, Veronese M, Rockers E, Bradbury K, Yu M, Nakawah MO, Román GC, Schulz PE, Arumanayagam AS, Beers D, Faridar A, Fujita M, Appel SH, Masdeu JC. Neuroinflammation is highest in areas of disease progression in semantic dementia. Brain. 2021;144:1565–75.
109. Vellas B, Carrillo MC, Sampaio C, Brashear HR, Siemers E, Hampel H, Schneider LS, Weiner M, Doody R, Khachaturian Z, Cedarbaum J, Grundman M, Broich K, Giacobini E, Dubois B, Sperling R, Wilcock GK, Fox N, Scheltens P, Touchon J, Hendrix S, Andrieu S, Aisen P. Designing drug trials for Alzheimer's disease: what we have learned from the release of the phase III antibody trials: a report from the EU/US/CTAD Task Force. Alzheimers Dement. 2013;9:438–44.
110. Petersen RC, Aisen P, Boeve BF, Geda YE, Ivnik RJ, Knopman DS, Mielke M, Pankratz VS, Roberts R, Rocca WA, Weigand S, Weiner M, Wiste H, Jack CR Jr. Mild cognitive impairment due to Alzheimer disease in the community. Ann Neurol. 2013;74:199–208.
111. Mathis CA, Kuller LH, Klunk WE, Snitz BE, Price JC, Weissfeld LA, Rosario BL, Lopresti BJ, Saxton JA, Aizenstein HJ, McDade EM, Kamboh MI, DeKosky ST, Lopez OL. In vivo assessment of amyloid-beta deposition in nondemented very elderly subjects. Ann Neurol. 2013;73:751–61.
112. Monsell SE, Mock C, Roe CM, Ghoshal N, Morris JC, Cairns NJ, Kukull W. Comparison of symptomatic and asymptomatic persons with Alzheimer disease neuropathology. Neurology. 2013;80:2121–9.
113. Nelson PT, Head E, Schmitt FA, Davis PR, Neltner JH, Jicha GA, Abner EL, Smith CD, Van Eldik LJ, Kryscio RJ, Scheff SW. Alzheimer's disease is not "brain aging": neuropathological, genetic, and epidemiological human studies. Acta Neuropathol. 2011;121:571–87.
114. Perez-Nievas BG, Stein TD, Tai HC, Dols-Icardo O, Scotton TC, Barroeta-Espar I, Fernandez-Carballo L, de Munain EL, Perez J, Marquie M, Serrano-Pozo A, Frosch MP, Lowe V, Parisi JE, Petersen RC, Ikonomovic MD, Lopez OL, Klunk W, Hyman BT, Gomez-Isla T. Dissecting phenotypic traits linked to human resilience to Alzheimer's pathology. Brain. 2013;136:2510–26.
115. Mintun MA, Lo AC, Duggan Evans C, Wessels AM, Ardayfio PA, Andersen SW, Shcherbinin S, Sparks J, Sims JR, Brys M, Apostolova LG, Salloway SP, Skovronsky DM. Donanemab in early Alzheimer's disease. N Engl J Med. 2021;384:1691–704.

116. Sperling RA, Donohue MC, Raman R, Sun CK, Yaari R, Holdridge K, Siemers E, Johnson KA, Aisen PS, Team AS. Association of factors with elevated amyloid burden in clinically normal older individuals. JAMA Neurol. 2020;77(6):735–45.
117. Jonasson M, Wall A, Chiotis K, Saint-Aubert L, Wilking H, Sprycha M, Borg B, Thibblin A, Eriksson J, Sorensen J, Antoni G, Nordberg A, Lubberink M. Tracer kinetic analysis of (S)-(1)(8)F-THK5117 as a PET tracer for assessing tau pathology. J Nucl Med. 2016;57:574–81.
118. Johnson KA, Schultz A, Betensky RA, Becker JA, Sepulcre J, Rentz D, Mormino E, Chhatwal J, Amariglio R, Papp K, Marshall G, Albers M, Mauro S, Pepin L, Alverio J, Judge K, Philiossaint M, Shoup T, Yokell D, Dickerson B, Gomez-Isla T, Hyman B, Vasdev N, Sperling R. Tau positron emission tomographic imaging in aging and early Alzheimer disease. Ann Neurol. 2016;79:110–9.
119. Chien DT, Bahri S, Szardenings AK, Walsh JC, Mu F, Su MY, Shankle WR, Elizarov A, Kolb HC. Early clinical PET imaging results with the novel PHF-tau radioligand [F-18]-T807. J Alzheimers Dis. 2013;34:457–68.
120. Fleisher AS, Pontecorvo MJ, Devous MD Sr, Lu M, Arora AK, Truocchio SP, Aldea P, Flitter M, Locascio T, Devine M, Siderowf A, Beach TG, Montine TJ, Serrano GE, Curtis C, Perrin A, Salloway S, Daniel M, Wellman C, Joshi AD, Irwin DJ, Lowe VJ, Seeley WW, Ikonomovic MD, Masdeu JC, Kennedy I, Harris T, Navitsky M, Southekal S, Mintun MA, Investigators AS. Positron emission tomography imaging with [18F]flortaucipir and postmortem assessment of Alzheimer disease neuropathologic changes. JAMA Neurol. 2020;77:829–39.
121. Scholl M, Lockhart SN, Schonhaut DR, O'Neil JP, Janabi M, Ossenkoppele R, Baker SL, Vogel JW, Faria J, Schwimmer HD, Rabinovici GD, Jagust WJ. PET imaging of tau deposition in the aging human brain. Neuron. 2016;89:971–82.
122. Marquie M, Normandin MD, Vanderburg CR, Costantino IM, Bien EA, Rycyna LG, Klunk WE, Mathis CA, Ikonomovic MD, Debnath ML, Vasdev N, Dickerson BC, Gomperts SN, Growdon JH, Johnson KA, Frosch MP, Hyman BT, Gomez-Isla T. Validating novel tau positron emission tomography tracer [F-18]-AV-1451 (T807) on postmortem brain tissue. Ann Neurol. 2015;78:787–800.
123. Hansen AK, Knudsen K, Lillethorup TP, Landau AM, Parbo P, Fedorova T, Audrain H, Bender D, Ostergaard K, Brooks DJ, Borghammer P. In vivo imaging of neuromelanin in Parkinson's disease using 18F-AV-1451 PET. Brain. 2016;139:2039–49.
124. Lowe VJ, Curran G, Fang P, Liesinger AM, Josephs KA, Parisi JE, Kantarci K, Boeve BF, Pandey MK, Bruinsma T, Knopman DS, Jones DT, Petrucelli L, Cook CN, Graff-Radford NR, Dickson DW, Petersen RC, Jack CR Jr, Murray ME. An autoradiographic evaluation of AV-1451 tau PET in dementia. Acta Neuropathol Commun. 2016;4:58.
125. Ikonomovic MD, Abrahamson EE, Price JC, Mathis CA, Klunk WE. [F-18]AV-1451 positron emission tomography retention in choroid plexus: more than "off-target" binding. Ann Neurol. 2016;80:307–8.
126. Ossenkoppele R, Schonhaut DR, Scholl M, Lockhart SN, Ayakta N, Baker SL, O'Neil JP, Janabi M, Lazaris A, Cantwell A, Vogel J, Santos M, Miller ZA, Bettcher BM, Vossel KA, Kramer JH, Gorno-Tempini ML, Miller BL, Jagust WJ, Rabinovici GD. Tau PET patterns mirror clinical and neuroanatomical variability in Alzheimer's disease. Brain. 2016;139:1551–67.
127. Taniguchi-Watanabe S, Arai T, Kametani F, Nonaka T, Masuda-Suzukake M, Tarutani A, Murayama S, Saito Y, Arima K, Yoshida M, Akiyama H, Robinson A, Mann DM, Iwatsubo T, Hasegawa M. Biochemical classification of tauopathies by immunoblot, protein sequence and mass spectrometric analyses of sarkosyl-insoluble and trypsin-resistant tau. Acta Neuropathol. 2016;131:267–80.
128. Smith R, Puschmann A, Scholl M, Ohlsson T, van Swieten J, Honer M, Englund E, Hansson O. 18F-AV-1451 tau PET imaging correlates strongly with tau neuropathology in MAPT mutation carriers. Brain. 2016;139:2372–9.
129. Josephs KA, Martin PR, Botha H, Schwarz CG, Duffy JR, Clark HM, Machulda MM, Graff-Radford J, Weigand SD, Senjem ML, Utianski RL, Drubach DA, Boeve BF, Jones DT,

Knopman DS, Petersen RC, Jack CR Jr, Lowe VJ, Whitwell JL. [(18) F]AV-1451 tau-PET and primary progressive aphasia. Ann Neurol. 2018;83:599–611.
130. Josephs K, Tosakulwong N, Weigand S, Buciuc M, Lowe V, Dickson D, Whitwell J. Relationship between (18)F-flortaucipir uptake and histologic lesion types in 4-repeat tauopathies. J Nucl Med. 2021;63(6):931–5.
131. Marquie M, Normandin MD, Meltzer AC, Siao Tick Chong M, Andrea NV, Anton-Fernandez A, Klunk WE, Mathis CA, Ikonomovic MD, Debnath M, Bien EA, Vanderburg CR, Costantino I, Makaretz S, DeVos SL, Oakley DH, Gomperts SN, Growdon JH, Domoto-Reilly K, Lucente D, Dickerson BC, Frosch MP, Hyman BT, Johnson KA, Gomez-Isla T. Pathologic correlations of [F-18]-AV-1451 imaging in non-Alzheimer tauopathies. Ann Neurol. 2016;81(1):117–28.
132. Harrison TM, Ward TJ, Murphy A, Baker SL, Dominguez PA, Koeppe R, Vemuri P, Lockhart SN, Jung Y, Harvey DJ, Lovato L, Toga AW, Masdeu J, Oh H, Gitelman DR, Aggarwal N, Snyder HM, Baker LD, DeCarli C, Jagust WJ, Landau SM. Optimizing quantification of MK6240 tau PET in unimpaired older adults. NeuroImage. 2023;265:119761.
133. Tezuka T, Takahata K, Seki M, Tabuchi H, Momota Y, Shiraiwa M, Suzuki N, Morimoto A, Nakahara T, Iwabuchi Y, Miura E, Yamamoto Y, Sano Y, Funaki K, Yamagata B, Ueda R, Yoshizaki T, Mashima K, Shibata M, Oyama M, Okada K, Kubota M, Okita H, Takao M, Jinzaki M, Nakahara J, Mimura M, Ito D. Evaluation of [(18)F]PI-2620, a second-generation selective tau tracer, for assessing four-repeat tauopathies. Brain Commun. 2021;3:fcab190.
134. Rullmann M, Brendel M, Schroeter ML, Saur D, Levin J, Perneczky RG, Tiepolt S, Patt M, Mueller A, Villemagne VL, Classen J, Stephens AW, Sabri O, Barthel H, On Behalf of the German Imaging Initiative for Tauopathies Gii T. Multicenter (18)F-PI-2620 PET for in vivo Braak staging of tau pathology in Alzheimer's disease. Biomol Ther. 2022;12(3):458.
135. Schönecker S, Palleis C, Franzmeier N, Katzdobler S, Ferschmann C, Schuster S, Finze A, Scheifele M, Prix C, Fietzek U, Weidinger E, Nübling G, Vöglein J, Patt M, Barthel H, Sabri O, Danek A, Höglinger GU, Brendel M, Levin J. Symptomatology in 4-repeat tauopathies is associated with data-driven topology of [(18)F]-PI-2620 tau-PET signal. Neuroimage Clin. 2023;38:103402.
136. Wang L, Benzinger TL, Su Y, Christensen J, Friedrichsen K, Aldea P, McConathy J, Cairns NJ, Fagan AM, Morris JC, Ances BM. Evaluation of tau imaging in staging Alzheimer disease and revealing interactions between beta-amyloid and tauopathy. JAMA Neurol. 2016;73:1070–7.
137. Nelson PT, Alafuzoff I, Bigio EH, Bouras C, Braak H, Cairns NJ, Castellani RJ, Crain BJ, Davies P, Del Tredici K, Duyckaerts C, Frosch MP, Haroutunian V, Hof PR, Hulette CM, Hyman BT, Iwatsubo T, Jellinger KA, Jicha GA, Kovari E, Kukull WA, Leverenz JB, Love S, Mackenzie IR, Mann DM, Masliah E, McKee AC, Montine TJ, Morris JC, Schneider JA, Sonnen JA, Thal DR, Trojanowski JQ, Troncoso JC, Wisniewski T, Woltjer RL, Beach TG. Correlation of Alzheimer disease neuropathologic changes with cognitive status: a review of the literature. J Neuropathol Exp Neurol. 2012;71:362–81.
138. Groot C, Doré V, Robertson J, Burnham SC, Savage G, Ossenkoppele R, Rowe CC, Villemagne VL. Mesial temporal tau is related to worse cognitive performance and greater neocortical tau load in amyloid-β-negative cognitively normal individuals. Neurobiol Aging. 2021;97:41–8.
139. Ferretti MT, Cuello AC. Does a pro-inflammatory process precede Alzheimer's disease and mild cognitive impairment? Curr Alzheimer Res. 2011;8:164–74.
140. Serrano-Pozo A, Mielke ML, Gomez-Isla T, Betensky RA, Growdon JH, Frosch MP, Hyman BT. Reactive glia not only associates with plaques but also parallels tangles in Alzheimer's disease. Am J Pathol. 2011;179:1373–84.
141. Hoozemans JJ, Rozemuller AJ, van Haastert ES, Eikelenboom P, van Gool WA. Neuroinflammation in Alzheimer's disease wanes with age. J Neuroinflammation. 2011;8:171.

142. Maeda J, Zhang MR, Okauchi T, Ji B, Ono M, Hattori S, Kumata K, Iwata N, Saido TC, Trojanowski JQ, Lee VMY, Staufenbiel M, Tomiyama T, Mori H, Fukumura T, Suhara T, Higuchi M. In vivo positron emission tomographic imaging of glial responses to amyloid-beta and tau pathologies in mouse models of Alzheimer's disease and related disorders. J Neurosci. 2011;31:4720–30.
143. Okello A, Edison P, Archer HA, Turkheimer FE, Kennedy J, Bullock R, Walker Z, Kennedy A, Fox N, Rossor M, Brooks DJ. Microglial activation and amyloid deposition in mild cognitive impairment: a PET study. Neurology. 2009;72:56–62.
144. Kreisl WC, Fujita M, Fujimura Y, Kimura N, Jenko KJ, Kannan P, Hong J, Morse CL, Zoghbi SS, Gladding RL, Jacobson S, Oh U, Pike VW, Innis RB. Comparison of [(11)C]-(R)-PK 11195 and [(11)C]PBR28, two radioligands for translocator protein (18 kDa) in human and monkey: implications for positron emission tomographic imaging of this inflammation biomarker. NeuroImage. 2010;49:2924–32.
145. Fujita M, Kobayashi M, Ikawa M, Gunn RN, Rabiner EA, Owen DR, Zoghbi SS, Haskali MB, Telu S, Pike VW, Innis RB. Comparison of four (11)C-labeled PET ligands to quantify translocator protein 18 kDa (TSPO) in human brain: (R)-PK11195, PBR28, DPA-713, and ER176-based on recent publications that measured specific-to-non-displaceable ratios. EJNMMI Res. 2017;7:84.
146. Masdeu JC, Pascual B, Fujita M. Imaging neuroinflammation in neurodegenerative disorders. J Nucl Med. 2022;63:45S–52S.
147. Zou J, Tao S, Johnson A, Tomljanovic Z, Polly K, Klein J, Razlighi QR, Brickman AM, Lee S, Stern Y, Kreisl WC. Microglial activation, but not tau pathology, is independently associated with amyloid positivity and memory impairment. Neurobiol Aging. 2020;85:11–21.
148. Fan Z, Dani M, Femminella GD, Wood M, Calsolaro V, Veronese M, Turkheimer F, Gentleman S, Brooks DJ, Hinz R, Edison P. Parametric mapping using spectral analysis for (11)C-PBR28 PET reveals neuroinflammation in mild cognitive impairment subjects. Eur J Nucl Med Mol Imaging. 2018;45:1432–41.
149. Parbo P, Ismail R, Sommerauer M, Stokholm MG, Hansen AK, Hansen KV, Amidi A, Schaldemose JL, Gottrup H, Braendgaard H, Eskildsen SF, Borghammer P, Hinz R, Aanerud J, Brooks DJ. Does inflammation precede tau aggregation in early Alzheimer's disease? A PET study. Neurobiol Dis. 2018;117:211–6.
150. Kreisl WC, Lyoo CH, McGwier M, Snow J, Jenko KJ, Kimura N, Corona W, Morse CL, Zoghbi SS, Pike VW, McMahon FJ, Turner RS, Innis RB. In vivo radioligand binding to translocator protein correlates with severity of Alzheimer's disease. Brain. 2013;136:2228–38.
151. Fan Z, Brooks DJ, Okello A, Edison P. An early and late peak in microglial activation in Alzheimer's disease trajectory. Brain. 2017;140:792–803.
152. Pascoal TA, Benedet AL, Ashton NJ, Kang MS, Therriault J, Chamoun M, Savard M, Lussier FZ, Tissot C, Karikari TK, Ottoy J, Mathotaarachchi S, Stevenson J, Massarweh G, Scholl M, de Leon MJ, Soucy JP, Edison P, Blennow K, Zetterberg H, Gauthier S, Rosa-Neto P. Microglial activation and tau propagate jointly across Braak stages. Nat Med. 2021;27:1592–9.
153. Goker-Alpan O, Masdeu JC, Kohn PD, Ianni A, Lopez G, Groden C, Chapman MC, Cropp B, Eisenberg DP, Maniwang ED, Davis J, Wiggs E, Sidransky E, Berman KF. The neurobiology of glucocerebrosidase-associated parkinsonism: a positron emission tomography study of dopamine synthesis and regional cerebral blood flow. Brain. 2012;135:2440–8.